

INFLUENCE OF TMT ON FRACTURE PROPERTIES OF ALUMINUM ALLOYS

K. Welpmann*, G. Lütjering** and W. Bunk*

INTRODUCTION

It is possible to improve the mechanical properties of age-hardenable aluminum alloys by thermomechanical treatment (TMT), i.e. a combination of deformation and heat treatment. Numerous combinations of deformation and aging have been tried including deformation at elevated temperatures [1] or deformation after a pre-overaging treatment [2]. The final step of a TMT is always an aging treatment to achieve precipitation hardening. The reason for the improvement of mechanical properties is not always clearly understood but is mostly due to optimizing grain shape and size [3,4], introducing a homogeneous distribution of dislocations [1,5], or achieving a better distribution of precipitated particles.

In the peak hardened condition these high strength aluminum alloys exhibit pronounced precipitate-free zones (PFZ) along grain boundaries [6] leading to intergranular fracture [7]. In the present work the influence of cold working prior to aging (TMT) on this fracture mode was investigated. A pure version of the commercial 7075 aluminum alloy was used to avoid the influence of small Cr-rich inclusions on grain shape and fracture mode.

EXPERIMENTAL PROCEDURES

The composition of the alloy investigated was 5.65 wt.-% Zn, 2.50% Mg, 1.50% Cu, 0.003% Si and <0.003% Fe. The alloy was supplied by the Schweizerische Aluminium AG, Neuhausen, Switzerland, in form of 21 mm thick plate. After homogenization at 465°C for 30 minutes the grain size was about 180 μm . Because of the low Si and Fe content and the absence of Cr almost no inclusions were present in this alloy.

The thermomechanical treatment was performed by rolling at room temperature immediately after quenching in ice-water from the homogenization temperature of 465°C. The deformation degree was varied between $\varphi = 0$ and $\varphi = 0.5$. After an intermediate room temperature aging of about 3 days the final aging treatment was carried out at 160°C for various times.

The influence of the TMT on various mechanical properties was evaluated. Tensile tests were carried out on round specimens with a diameter of 6 mm and a gauge length of 25 mm. The strain rate was $6.7 \times 10^{-4} \text{s}^{-1}$. Fatigue life tests were conducted on round electrolytically polished specimens (diameter 4 mm) under push-pull loading at constant stress amplitudes with a frequency of 110 Hz. For the fracture toughness tests standard three point bend specimens were used with a thickness of 12.7 mm. The crack plane orientation was L-T with respect to the rolling direction.

*Deutsche Forschungs- und Versuchsanstalt für Luft- und Raumfahrt e. V., Institut für Werkstoff-Forschung, Köln, Germany.

**Ruhr-Universität Bochum, Institut für Werkstoffe, Bochum, Germany.

The fatigue crack propagation measurements were performed in vacuum under pulsating tensile loads (frequency 30 Hz, $R = 0.1$) on modified CT specimens with $B = 12.7$ mm and $W = 66.7$ mm. The test procedure for the stress corrosion investigations was the constant strain rate method. Round electrolytically polished specimens with diameter of 3.5 mm and gauge length of 20 mm were pulled in 3.5% NaCl solution at different strain rates.

The different microstructures and fracture surfaces were examined by TEM and SEM, respectively.

RESULTS

Initial Microstructures

The characteristic features of the microstructure developing upon aging at 160°C are illustrated in Figure 1. Within the matrix metastable particles are precipitated whereas at grain boundaries particles of the equilibrium phase appear. The dominant feature of the microstructure is the formation of narrow precipitate free zones (PFZ) along grain boundaries.

The characteristic structure modifications by TMT are shown in Figure 2. The rolling causes the formation of intense slip bands covering the whole matrix (Figure 2a). These slip bands often produce shear-offsets at grain boundaries (Figure 2b) which are also detectable by light microscopy. The subsequent aging at 160°C produces nearly the same particle distribution within the matrix and grain boundary regions as compared to the condition without TMT.

Tensile Properties

The main effects of TMT on the tensile properties are illustrated in Figure 3 comparing specimens without TMT ($\phi = 0$) and specimens with a cold rolling degree of $\phi = 0.5$. With increasing aging time at 160°C the yield stress measured after 0.2% plastic strain goes through a maximum which is slightly shifted to lower aging times by TMT. A drastic effect of TMT was found on the ductility. Whereas without TMT the true fracture strain goes through a pronounced minimum ($\epsilon_F = 0.13$) specimens with TMT exhibit always ductility values higher than $\epsilon_F = 0.45$. To explain this different behaviour the deformation and fracture mechanisms were investigated. The specimens without TMT deform preferentially within the PFZ along grain boundaries (Figure 4a). This preferred plastic deformation was also proved by light microscopy through surface marker displacements. Cracks are nucleated within these highly deformed regions either at grain boundary triple points or at the incoherent particles within the grain boundaries. It was found that the cracks propagate intercrystalline as may be seen from the fracture surface appearance (Figure 4b). At high magnification small dimples caused by the grain boundary particles are visible on the flat grain surfaces (Figure 4c).

In the TMT condition no extensive preferential plastic deformation along grain boundaries was found for tensile specimens. Also no pronounced modification in the starting slip band structure stemming from the cold rolling (Figure 2a) was observed. At high plastic strains close to macroscopic failure void formation at intersecting slip bands could be detected (Figure 5a). The investigation of the fracture surface revealed nearly a complete dimple type of fracture mode with only few grain surfaces present (Figure 5b). Observation at high magnification showed that

for most areas the dimple size (Figure 5c) can be correlated to the dimensions of the slip band structure (Figure 2a).

The influence of TMT on other mechanical properties was investigated for two treatments: $\phi = 0$, 8h at 160°C and $\phi = 0.5$, 4h at 160°C.

Fracture Toughness Tests

Comparing the two conditions mentioned above the K_Q and K_{max} values increased by TMT from 38.5 to 43.6 and from 40.7 to 56.4 $\text{MPa}\cdot\text{m}^{1/2}$, respectively. In analogy to the tensile tests the investigation of the fracture surfaces showed a change in crack propagation mechanism from an intercrystalline fracture mode for specimens without TMT (Figure 4b) to a transcrystalline dimple type of fracture for specimens with TMT (Figure 5b).

S-N Curves

Figure 6 shows the measured S-N curves for the two conditions investigated. It can be seen that the TMT increased the life time at high stress amplitudes but did not have a measurable influence on the fatigue strength. Light microscopic investigation of the specimen surfaces as a function of cycles indicated that a difference in crack nucleation period was responsible for the improvement of fatigue life by TMT at high stress amplitudes. In specimens without TMT the cracks nucleated at grain boundaries whereas in the TMT specimens cracks started in the matrix at large inclusions.

Fatigue Crack Propagation Measurements

The crack propagation rate da/dN as a function of cyclic stress intensity factor ΔK is plotted in Figure 7 for the two conditions investigated. At high ΔK values the specimens with TMT exhibited slower propagation rates in agreement with the measured K_Q values from the fracture toughness tests which are indicated by arrows in Figure 7. The investigation of the fracture surfaces showed basically the same results obtained for tensile and fracture toughness tests, i.e. intercrystalline crack propagation for specimens without TMT and transcrystalline crack propagation for specimens with TMT. At lower ΔK values the crack propagated faster in specimens with TMT (Figure 7). In this region both alloy conditions exhibited a fracture along slip bands as may be seen from the micrographs in Figure 8. This fracture along slip bands was much more pronounced for TMT specimens (Figure 8b) as compared to specimens without TMT (Figure 8a).

Stress Corrosion Tests

Due to the fact that only the constant strain rate method was available for the stress corrosion experiments the results of the tests should be taken only as a qualitative indication. Pulling specimens of the two conditions mentioned above at a strain rate of $\dot{\epsilon} = 4 \times 10^{-7} \text{s}^{-1}$ in a 3.5% NaCl solution gave the following results: The specimens without TMT fractured after a true strain of 0.16 whereas the specimens with TMT exhibited a value of $\epsilon_F = 0.65$. Comparing these results with the values obtained on laboratory air (Figure 3) it can be noticed that the ductility of the specimens without TMT declined in the salt solution whereas the ductility of the TMT specimens increased. The investigation of the fracture surfaces indicated that the tendency for intercrystalline fracture increased for the specimens without TMT. No visible changes in the dimple type of fracture surfaces could be detected for the specimens with TMT.

DISCUSSION

The low tensile ductility in the minimum of the age hardening curve at 160°C of the Al Zn Mg Cu alloy (Figure 3, minimum $\epsilon_F = 0.13$) is due to preferential plastic deformation within the weak precipitate-free zones along grain boundaries. These high local strains lead to crack nucleation within these regions and to a ductile intercrystalline fracture mode (Figure 4). The macroscopic ductility is then determined mainly by two parameters: The difference in yield stress between PFZ and age-hardened matrix and the grain boundary length, i.e. grain size [8]. By the TMT employed in this work namely cold rolling before aging at 160°C, the grain boundaries are disturbed by shear-offsets (Figure 2b) which limit the effective grain boundary length for preferential deformation during subsequent tensile straining. The stress concentrations within the grain boundary regions are thus reduced and crack nucleation in these regions will not occur at low macroscopic strains. Cracks are nucleated within the matrix (Figure 5a) and the fracture is a transcrystalline dimple type of fracture mode (Figures 5b and 5c). The tensile ductility of the alloy is therefore drastically increased by TMT (Figure 3, ϵ_F : 0.13 to 0.45).

The TMT employed also improves other mechanical properties, namely fracture toughness, fatigue life (Figure 6), fatigue crack propagation rate in vacuum at high ΔK values (Figure 7), and stress corrosion resistance. One exception was observed: The fatigue crack propagation rate in vacuum was increased by the TMT at low and medium ΔK values (Figure 7). From the corresponding fracture surfaces an explanation for this behaviour can be deduced. The alloy exhibits normally, i.e. without TMT, at low fatigue crack propagation rates no intercrystalline fracture but a fracture along slip bands (Figure 8a) [9]. Since in the TMT condition pronounced slip bands are already present due to the cold rolling (Figure 2a) the crack propagates much faster as compared to specimens without TMT.

Generally it can be said that the TMT employed in this work will improve the mechanical properties of aluminum alloys if without TMT the mechanism of preferential deformation within PFZ leading to an intercrystalline fracture determines the mechanical properties.

REFERENCES

1. PATON, N. E. and SOMMER, A. W., Proc. of Third Int. Conf. on Strength of Metals and Alloys, Cambridge, 1973, Vol. 1, 101.
2. THOMPSON, D. S., LEVY, S. A. and BENSON, D. K., Proc. of Third Int. Conf. on Strength of Metals and Alloys, Cambridge, 1973, Vol. 1, 119.
3. DI RUSSO, E., CONSERVA, M., BURATTI, M. and GATTO, F., Mat. Sci. Eng. 14, 1974, 23.
4. WALDMAN, J., SULINSKI, H. and MARKUS, H., Met. Trans., 5, 1974, 573.
5. OSTERMANN, F., Met. Trans., 2, 1971, 2897.
6. STARKE, E. A., J. Metals, 22, 1970, No. 1, 54.
7. WELPMANN, K., LÜTJERING, G. and BUNK, W., Aluminium, 50, 1974, 263.
8. PETERS, M. and LÜTJERING, G., to be published in Z. Metallkunde, 1976.
9. ALBRECHT, J., MARTIN, J. W. R., LÜTJERING, G. and MARTIN, J. W., Proc. of Fourth Int. Conf. on Strength of Metals and Alloys, Nancy, France, 1976.

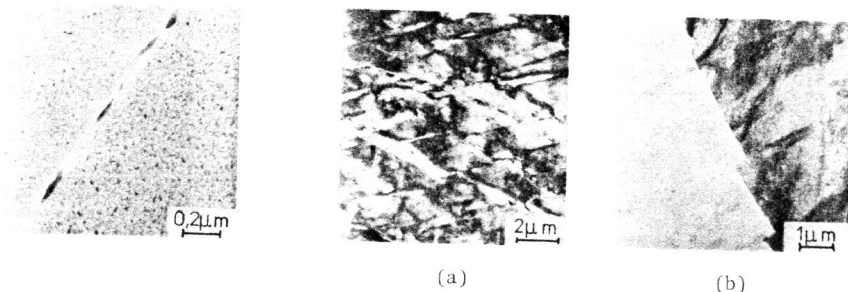


Figure 1 $\phi = 0$, 48h 160°C. Microstructure of the Alloy without TMT (TEM)

Figure 2 $\phi = 0.5$, 4h 160°C. Microstructural Modifications by TMT (TEM). (a) Slip Band Structure, (b) Shear-Offsets at Grain Boundaries

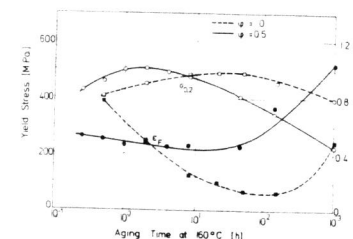


Figure 3 Yield Stress $\sigma_{0.2}$ and True Fracture Strain, ϵ_F versus Aging Time at 160°C for Specimens without TMT ($\phi = 0$) and with TMT ($\phi = 0.5$)

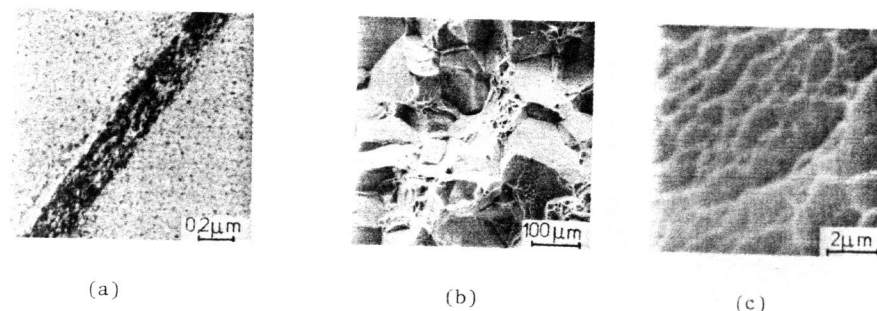


Figure 4 $\phi = 0$, 48h 160°C, Tensile Tests. Deformation and Fracture Mechanisms of the Alloy without TMT. (a) $\epsilon = 0.1$, Preferred Deformation within PFZ (TEM), (b) $\epsilon_F = 0.14$, Intercrystalline Fracture (SEM), (c) $\epsilon_F = 0.14$, Dimples on Grain Boundary Surface (SEM)

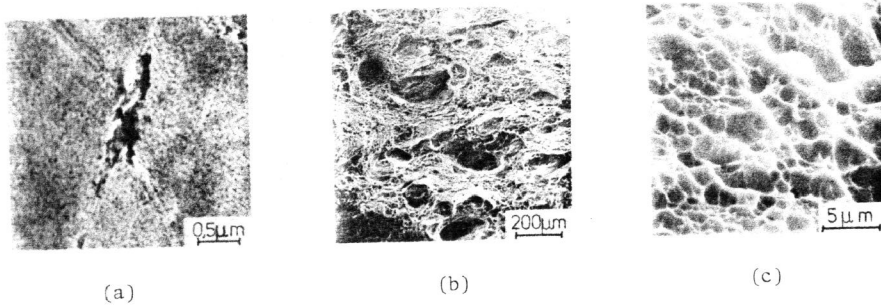


Figure 5 $\phi = 0.5$, 160°C , Tensile Tests. Deformation and Fracture Mechanisms of the TMT Condition. (a) 45h 160°C , $\epsilon = 0.4$. Void Formation at the Intersecting Slip Bands (TEM), (b) 4h 160°C , $\epsilon_F = 0.45$. Transcrystalline Fracture (SEM), (c) 4h 160°C , $\epsilon_F = 0.45$. Dimples on Transcrystalline Fracture Surface (SEM)

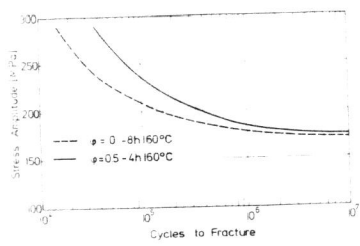


Figure 6 S-N Curves for the Two Alloy Conditions Investigated

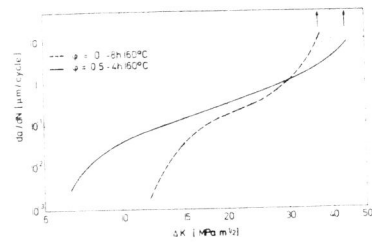
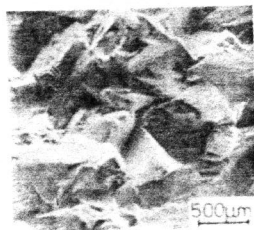
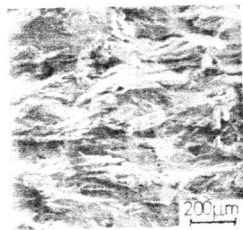


Figure 7 Fatigue Crack Propagation Rate da/dN in Vacuum versus Cyclic Stress Intensity Factor ΔK



(a)



(b)

Figure 8 Fracture Surface of Fatigue Crack Propagation Specimens of the Two Alloy Conditions Investigated. Fracture Along Slip Bands at $da/dN = 0.01 \mu\text{m}/\text{cycle}$ (SEM). (a) Condition Without TMT, $\Delta K = 13.5 \text{ MPa m}^{1/2}$, (b) TMT Condition, $\Delta K = 7.5 \text{ MPa m}^{1/2}$